IEEE Access
Multidisciplinary | Rapid Review | Open Access Journal

Received June 17, 2019, accepted June 26, 2019, date of publication July 1, 2019, date of current version July 15, 2019.

Digital Object Identifier 10.1109/ACCESS.2019.2926100

Fault Diagnosis of High-Voltage Circuit Breakers Using Mechanism Action Time and Hybrid Classifier

SHUTING WAN AND LEI CHEN
Department of Mechanical Engineering, North China Electric Power University, Baoding 071003, China
Corresponding author: Lei Chen (chenlei@ncepu.edu.cn)

ABSTRACT Accurate fault diagnosis of high-voltage circuit breakers is crucial for the safety of power grids. Mechanism action time, though can reflect the state of high-voltage circuit breakers, is usually difficult to obtain, as multiple sensors are required for acquisition. To solve this problem, a novel method that can extract mechanism action time from vibration signals was proposed in this paper. The method involved enhancement of vibration signals using short-time zero-crossing rate and determination of mechanism action time by the double threshold method. Then, time parameters were utilized to calculate singular spectrum entropy as the input vector for a classifier. Finally, a hybrid classifier that involved support vector data description and extreme learning machine was developed to identify faults. The hybrid classifier can not only classify known mechanical states but also detect unknown mechanical faults of high-voltage circuit breakers. The effectiveness of the proposed method was verified using a 35-kV high-voltage circuit breaker.

INDEX TERMS Fault diagnosis, circuit breakers, motion estimation, time measurement, vibration measurement, signal processing, entropy, pattern recognition.

I. INTRODUCTION

High-voltage circuit breakers (HVCBs) directly affect the stability and safety of the power system as it is one of the important control components in a high voltage circuit [1], [2]. Previous study has reported that the vast majority of faults of HVCBs are mechanical faults [3]. As a result, it is necessary to monitor mechanical states of HVCBs so as to maintain the power grid [4], [5]. In general, the mechanism action time can effectively reflect the state of HVCBs. However, the mechanism action time, though effective, is usually extracted from multiple signals, which requires multiple sensors to collect the signals. Thus there is the need to install sensors at each static contact to measure the arrival and departure time of the moving contact, and also the need to collect current signals to measure the action time of HVCBs. Therefore, in order to find a more simpler method for mechanical fault diagnosis of HVCBs, significant research efforts have been devoted to process various signals such as coil current, contact displacement, acoustic signals, and vibration signals for monitoring condition over recent years [6]. Mei *et al.* [7] developed a hybrid fault diagnostic model for HVCBs by using electromagnet coil current information, and the result showed that the model could correctly identify faults of HVCBs. Moreover, Forootani *et al.* [8] constructed a dynamic model to track changes in the contact displacement and finally realized the detection of early faults of HVCBs. Yang *et al.* [9] realized faults diagnosis of HVCBs based on acoustic signals by searching different intervals of amplitude between the normal signal and fault signal. Huang *et al.* [10] constructed a hybrid classifier to identify faults of HVCBs based on feature vectors extracted from vibration signals. Among all the signals being currently used for the extraction of fault-related features of HVCBs, the vibration signal is the most used signal due to its convenience of acquisition [11]. Waveforms of vibration signals of various faults are similar but fault features may exist in different frequency components; therefore, multi-scale decomposition methods such as empirical mode decomposition (EMD), empirical wavelet transform (EWT), wavelet packet transform (WPT), and variational mode decomposition (VMD) have been applied to decompose vibration signals for extraction of features. After the decomposition, a vibration signal can be transformed into several intrinsic mode functions (IMFs). Liu *et al.* [12] applied EMD method on vibration

The associate editor coordinating the review of this manuscript and approving it for publication was Gerard-Andre Capolino.

signals and then extracted feature vectors from selected IMFs. Li *et al.* [13] employed EWT method to decompose vibration signals and then extracted time-frequency entropy as feature vectors. Ji *et al.* [14] decomposed the vibration signal into different frequency bands by WPT. Then sample entropy in low frequency band and energy in high frequency band were calculated as feature vectors respectively. Huang *et al.* [15] extracted feature vectors from the IMFs decomposed by VMD for the diagnosis of HVCBs. Although these studies have achieved good diagnostic results, the above mentioned decomposition methods are subjected to disadvantages including energy leakage, endpoint effect, and randomness of the determination of decomposition levels, which may affect the robustness of diagnostic results. Moreover, these decomposition methods require considerable time to implement, which does not meet the requirement of real-time monitoring.

Considering that a vibration signal recorded using an acceleration sensor is the reflection of motions of structures involved in operating mechanism [16], starting time and ending time of some major vibration events such as motion of the cam and collision of the moving contact and the static contact may be extracted from vibration signals. Inspired by the endpoint detection method used in the processing of a speech signal [17], short-time zero-crossing rate (STZCR) combined with double threshold method (DTM) was developed to extract time parameters from vibration signals in this study. With the help of time parameters, the time domain segmentation of a vibration signal was realized. Then singular spectrum entropy (SSE) was calculated as feature vectors.

After feature extraction, the key issue is to construct an effective classifier model. The support vector machine (SVM) [14]–[16], fuzzy C-mean (FCM) [18]–[20], back propagation neural network (BPNN) [21], [22], random forest (RF) method [6], [23], and generalized regression neural network (GRNN) [13] have been commonly applied in fault diagnosis of HVCBs. However, FCM is sensitive to noisy data and BPNN relies on considerable training dataset to ensure high recognition rate. SVM is greatly influenced by two parameters, namely, penalty coefficient and kernel function parameter [24], which may lead to a misjudgment of fault identification. RF method, though powerful, requires considerable time for training. As a new fast machine learning model, extreme learning machine (ELM) offers a fast learning speed and generalization ability. ELM is developed for single hidden layer feedforward neural networks (SLFNs). Different from BPNN, ELM can randomly initialize input weights and biases between the input layer and the hidden layer [25], [26]. Moreover, the connection weights and the neuron thresholds do not require adjustment during the training of ELM. Over the past years, ELM has been successfully used in fault classification and feature learning due to its superiority [27]. In this study, ELM was employed to classify faults of HVCBs.

Previous researches are mostly holding that all faults are known. However, recording all types of mechanical faults for the training of classifiers is unrealistic. Unknown faults are definitely identified as a known state. Therefore, performing identification of unknown faults is necessary. In this study, samples belonging to unknown faults were assumed as outliers, which could be identified by a one-class classifier. As a result, support vector data description (SVDD) [28] was employed to identify unknown faults. SVDD has many applications in fault diagnosis, which realizes the identification of unknown faults by constructing an optimal sphere. Whether the sample is located in the sphere is the basis for the distinction between known states and unknown faults.

This study proposed a novel approach for diagnosis of mechanical faults of HVCBs. STZCR combined with DTM was first used to extract parameters of mechanism action time from vibration signals. Then vibration signals were segmented into several segments by time parameters. Based on this, SSE was calculated as feature vectors for the training of the hybrid classifier that was composed of ELM and SVDD. Finally, identification of faults of HVCBs was realized by the hybrid classifier.

The remaining sections of this paper are arranged as follows. Section II introduces the research framework, which contains the process of fault diagnosis, techniques for feature extraction, and fault identification. Section III describes the experimental setup and measurement procedures. Results and analysis of experiments are presented in Section IV. Finally, Section V highlights the conclusions.

II. RESEARCH FRAMEWORK

A. FAULT DIAGNOSIS PROCESS

As a complicated mechanical system, different mechanical faults of HVCBs are always holding similar features. To extract more useful features of faults, mechanism action time parameters extracted from vibration signals were used to segment vibration signals into smaller segments, and then SSE was extracted as feature vectors from the segments. Finally, SVDD was trained to identify unknown faults while ELM was trained to classifier known states. The process of the approach proposed for the fault diagnosis of HVCBs is shown in Fig. 1, which is composed of the following three parts: data acquisition, feature extraction, and faults identification.

B. ANALYSIS OF MECHANISM ACTION TIME

The spring operating mechanism of an HVCB is a multi-link mechanism which uses stored energy of spring to realize operations of opening or closing [29]–[31]. The operating mechanism of an HVCB is linked with several structures [32], including the cam, rods, moving contact, arms, and insulating rod, as shown in Fig. 2. Operations of HVCBs were accomplished by sequential motions of these structures, thus recording action time parameters of main structures such as the cam and the moving contact can indirectly reflect the mechanical state of an HVCB. In this study, motion of the cam and collision of the moving contact and the static contact were designated as sub-events.

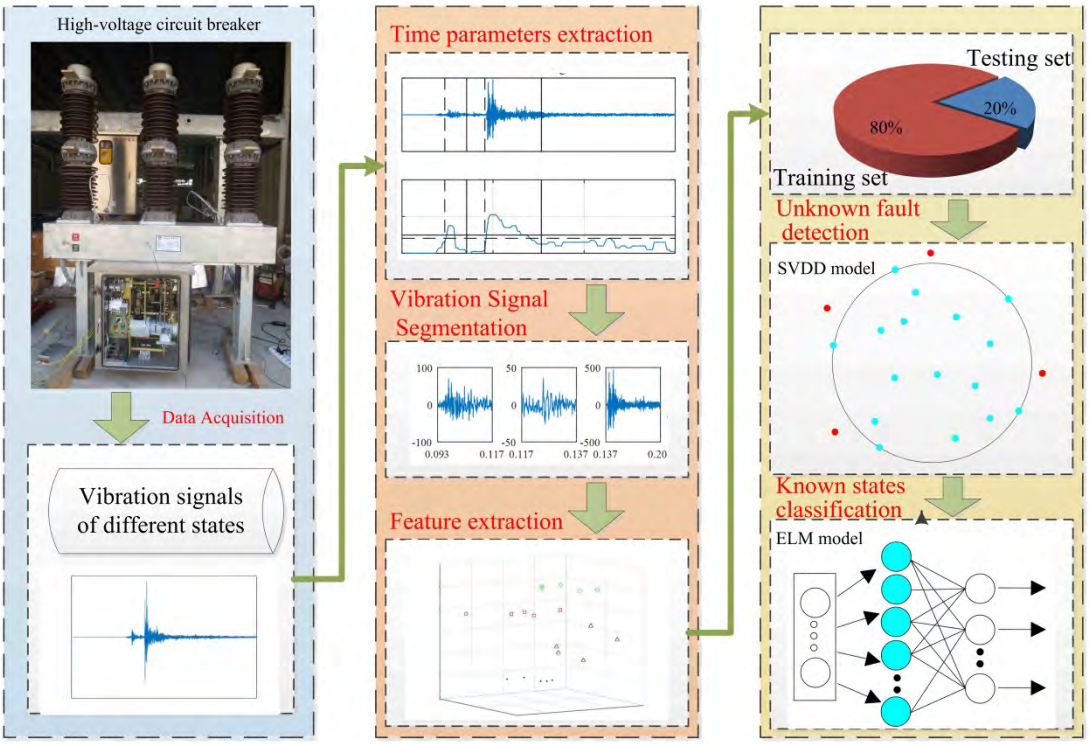

FIGURE 1. Fault diagnosis process of the proposed method.

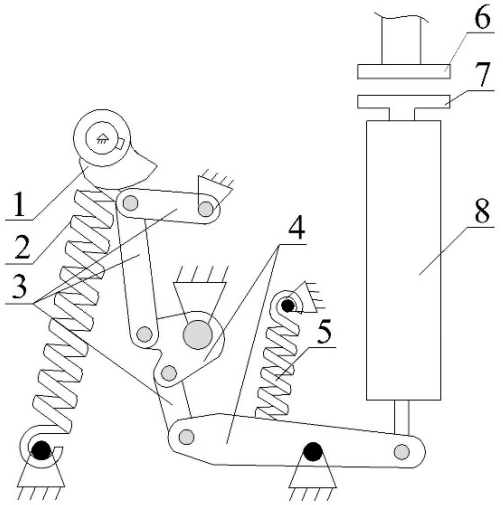

1-cam, 2-closing spring, 3-connecting rods, 4-inflective arms, 5-opening spring, 6-static contact, 7-moving contact, 8-insulated pull rod

FIGURE 2. Schematic illustration of the spring operating mechanism of HVCBs.

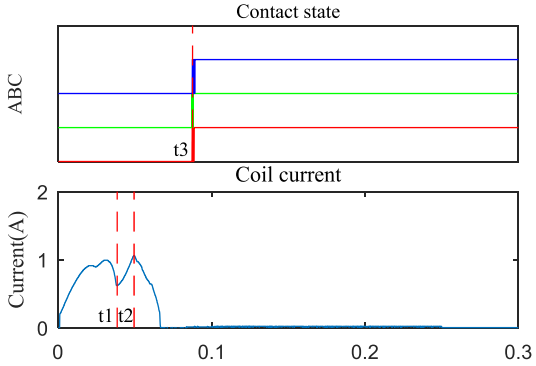

FIGURE 3. Actual time parameters of sub-events.

The actual starting time of the sub-events can be extracted from the coil current of the iron core and contact states of the moving contact, as shown in Fig. 3.

Moreover, the specific descriptions of the time parameters are as follows [33]–[35]:

Time 0 is the moment when the HVCB receives an action instruction.

T1: t1 is the moment when the iron core impacts the shackle, then, the spring operating mechanism starts working.

T2: t2 is the moment when the moving contact starts shifting.

T3: t3 is the moment when the moving contact reaches the position of the static contact.

When the iron core successfully knocks the lock, the operating mechanism starts working. Motions of structures of the operating mechanism cause vibration, in particular, the motion of the cam and the collision of the moving contact and the static contact. Correspondingly, vibration signals collected using an acceleration sensor during a process of the operation of HVBCs, are the superposition of vibration caused by structures of the operating mechanism. Since

motions of structures are sequential, time parameters may be extracted from vibration signals. Furthermore, compared to acquisition of coil current and contact state signals requires multiple sensors, the acquisition of vibration signals is more convenient as it only requires one sensor. Therefore, it will greatly reduce the complexity of fault diagnosis if the time parameters can be successfully extracted from vibration signals.

C. EXTRACTION OF MECHANISM ACTION TIME

To meet the requirement of fast breaking current, the action process of HVCBs is very quick. It is thus difficult to extract time parameters of sub-events. In this study, STZCR was used to enhance the feature of sub-events. Then DTM was used to extract time parameters. Before using STZCR, vibration signals should be split into multiple frames by a window function with defined length beforehand, which is called framing.

Assuming that a vibration signal is $x(t)$, after framing, the ith frame is shown as follows:

$$y_i(n) = \omega(n) * x((i-1) * inc + n) \tag{1}$$

where $\omega(n)$ is the window function, $y_i(n)$ is the ith frame of a vibration signal, $n = 1, 2, \ldots L$, $i = 1, 2 \ldots, fn$, inc is the shift length of framing, L is the length of the framed signal, and fn is the total number of the framed signal.

In this study, Hamming window function was adopted, which is defined as follows:

$$\omega(n) = \begin{cases} 0.54 - 0.46\cos(2\pi n/(L-1)) & 0 \le n \le L-1 \\ 0 & \text{otherwise} \end{cases} \tag{2}$$

1) SHORT-TIME ZERO-CROSSING RATE

STZCR stands for the frequency that a frame passes through the transverse axis, which is used to enhance the vibration signals and can be expressed as follows:

$$Z(i) = \frac{1}{2}\sum_{n=0}^{L-1} |\mathrm{sgn}[y_i(n)] - \mathrm{sgn}[y_i(n-1)]| \tag{3}$$

where,

$$\mathrm{sgn}[x] = \begin{cases} -1 & x < 0 \\ 1 & x \ge 0 \end{cases} \tag{4}$$

2) DOUBLE THRESHOLD METHOD

The DTM endpoint detection algorithm should set two thresholds for STZCR. The time parameters of a sub-event were detected by higher threshold while the lower threshold was used to accurately detect real-time parameters of a sub-event. The specific judgment process is shown in Fig. 4. Clearly, T1 is higher threshold, while T2 is lower threshold. Fig. 4 demonstrates that the AB and CD segments are definitely sub-events as they are higher than T1. Then both sides from AB and CD are searched to determine the starting time and ending time of sub-events at low thresholds.

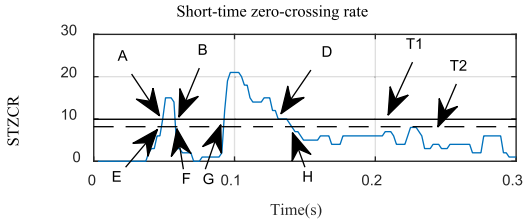

FIGURE 4. DTM for judging time parameters.

D. FEATURE EXTRACTION

Effective working of a classifier is directly influenced by feature vectors. There is a clearance in motion pairs of the operating mechanism; therefore, differences of time parameters may even exist in samples belonging to the same type of faults [36]. Thus, time parameters are unsuitable to be used as feature vectors directly. In this study, time parameters were used to segment vibration signals, and then feature vectors were calculated from segmented signals.

Singular spectrum analysis is an effective method for analyzing and predicting non-linear time series [37], which is thus suitable to mine the essence of vibration signals. In this study, SSE was calculated as feature vectors of vibration signals of HVCBs.

First, n-dimensional phase space was reconstructed. Assuming that the signal to be reconstructed is $x(i)$, the reconstruction result is as follows:

$$A_{(N-n+1)\times n} = \begin{bmatrix} x(1) & x(2) & \cdots & x(n) \\ x(2) & x(3) & \cdots & x(n+1) \\ \vdots & \vdots & \vdots & \vdots \\ x(N-n+1) & x(N-n+1) & \cdots & x(N) \end{bmatrix} \tag{5}$$

Then the matrix A is decomposed by singular value decomposition (SVD):

$$A = U_{(N-n+1)\times l} S_{l\times l} V^{\mathrm{T}}_{l\times l} \tag{6}$$

where nonzero diagonal elements $\lambda(i)$ of $S_{l\times l}$ are called singular values.

SSE is calculated as follows:

$$H_{SSE}(k) = -\sum_{i=1}^{n} q(i)\ln q(i) \tag{7}$$

where,

$$q(i) = \frac{\lambda(i)}{\sum_{i=1}^{n}\lambda(i)} \tag{8}$$

E. HYBRID CLASSIFIER

1) PRINCIPLES OF EXTREME LEARNING MACHINE

As a new fast machine learning algorithm, ELM is developed for SLFNs and can randomly initialize input weights and biases [38]. Fig. 5 shows the principle of ELM.

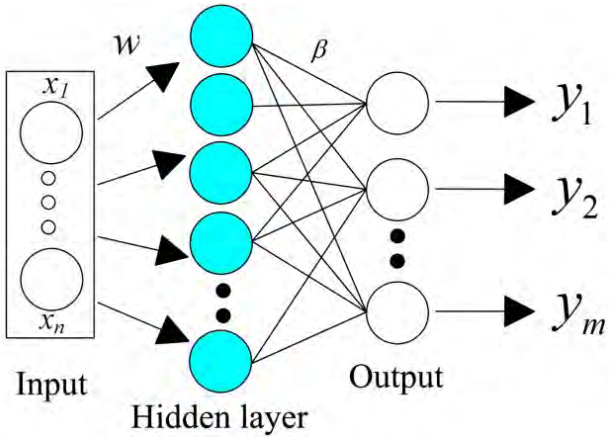

FIGURE 5. The principle of ELM.

Assuming that there is a training set $\{(x_j, t_j)|x_j \in \mathrm{R}^n, t_j \in \mathrm{R}^m\}$, thus an SLFN with l hidden nodes can be defined as follows:

$$y_j = \sum_{i=1}^{l} \beta_i g(w_i \cdot x_j + b_i) \quad j = 1, 2, \cdots, M \tag{9}$$

where x_j represents the input feature vector of the jth sample, t_j represents the desired output label of the jth sample, $w_i = [w_{i1}, w_{i2}, \cdots, w_{in}]^{\mathrm{T}}$ represents the input weight that connects the ith hidden node and input nodes, b_i represents the bias value of the ith hidden node, y_j represents the output of the ELM model of the jth sample, $g(\cdot)$ represents the activation function, and $\beta_i = [\beta_{i1}, \beta_{i2}, \cdots, \beta_{im}]^{\mathrm{T}}$ represents the output weight that connects the ith hidden node and output nodes.

If the outputs of the SLFN are consistent with the categories of samples, namely, $\sum_{j=1}^{M} \|y_j - t_j\| = 0$, then (9) can be transformed as follows:

$$\sum_{i=1}^{l} \beta_i g(w_i \cdot x_j + b_i) = t_j \quad j = 1, 2, \cdots, M \tag{10}$$

Equation (10) can be represented as:

$$H\beta = T \tag{11}$$

where,

$$H(w_1, w_2, \cdots, w_l, x_1, x_2, \cdots, x_M, b_1, b_2, \cdots, b_l) = \begin{bmatrix} g(w_1 \cdot x_1 + b_1) & \cdots & g(w_l \cdot x_l + b_l) \\ \vdots & \cdots & \vdots \\ g(w_1 \cdot x_M + b_1) & \cdots & g(w_l \cdot x_M + b_l) \end{bmatrix}_{M \times l} \tag{12}$$

$$\beta = [\beta_1, \beta_2, \cdots, \beta_l]^{\mathrm{T}}_{l \times m} \tag{13}$$

$$T = [t_1, t_2, \cdots, t_l]^{\mathrm{T}}_{M \times m} \tag{14}$$

where T represents classes of samples.

In order to have better generalized performance, a kernel function can be used to replace the active function $g(\cdot)$. In this study, Gaussian kernel function was adopted, which is defined as follows:

$$K(x_i, x_j) = \exp\left(\frac{\|x_i - x_j\|^2}{\sigma^2}\right) \tag{15}$$

where σ is the kernel width.

Thus the hidden layer output matrix can be rewritten as:

$$H = \begin{bmatrix} K(x_1, x_1) & \cdots & K(x_1, x_l) \\ \vdots & \cdots & \vdots \\ K(x_M, x_1) & \cdots & K(x_M, x_l) \end{bmatrix}_{M \times l} \tag{16}$$

The output weight vector β can be calculated as follows:

$$\beta = H^{+}T \tag{17}$$

where H^{+} represents the Moore–Penrose generalized inverse of matrix H, and T represents classes of samples.

2) PRINCIPLES OF SUPPORT VECTOR DATA DESCRIPTION

As a one-class classifier, SVDD has a good application in the detection of outliers. In this study, SVDD tries to find a sphere that can distinguish whether samples belong to known states or unknown faults, as shown in Fig. 6. Moreover, the sphere should contain samples belonging to known states as close as possible.

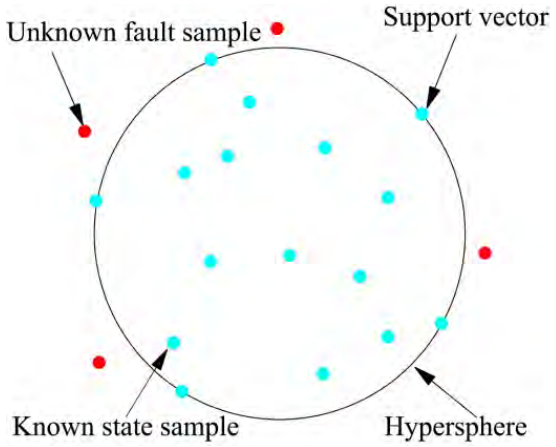

FIGURE 6. The principle of SVDD.

Assuming that the training samples are $Q = \{x_i| i = 1, \ldots, M\}$, then the sphere can be defined by [39]:

$$\begin{aligned} &\min f\ (r, a, \xi_i) = C \sum_{i}^{M} \xi_i + r^2 \\ &\text{s.t.}\ \|x_i - a\| \le r^2 + \xi_i, \xi_i \ge 0 \end{aligned} \tag{18}$$

where ξ_i is the slack variable, C is the penalty factor which aids in balancing the volume of the sphere against the quantity of samples that belong to unknown faults, r is the radius of the sphere, and a is center of the sphere.

Equation (18) can be solved by using the Lagrange multiplier method.

$$f(\alpha_i, r, a, \xi_i) = C\sum_{i}^{M}\xi_i + R^2 - \sum_{i}\gamma_i\xi_i - \sum_{i}\alpha_i\left[r^2 + \xi_i^2 - (x_i - a)^2\right],\ a_i > 0, \gamma_i \geq 0 \quad (19)$$

where α_i and γ_i are the Lagrange multipliers.

The kernel function is introduced to solve the above mentioned optimization problem:

$$\min f = \sum_{i}\alpha_i K(x_i, x_i) - \sum_{i,j}^{M}\alpha_i\alpha_j K(x_i, x_j)$$
$$\text{s.t. } 0 \leq \alpha_i \leq C, \sum_{i=1}^{M}\alpha_i = 1 \quad (20)$$

where $K(x_i,x_i)$ is radial basis function. Solving (20) can provide a set of Lagrange multipliers α_i. Moreover, samples x_i with $\alpha_i > 0$ are called support vectors, which are the points on the boundary of the sphere in Fig. 6.

The distance D from a sample to the center of the sphere is calculated as follows:

$$D = \sqrt{K(x, x) + \sum_{i=1}^{M}\sum_{j=1}^{M}\alpha_i\alpha_j K(x_i, x_j) - 2\sum_{i=1}^{M}\alpha_i K(x_i, x)} \quad (21)$$

Whether the sample is located in the sphere is the basis for the distinction between known states and unknown faults, which can be judged by:

$$f_{\text{svdd}} = \text{sgn}\left(r^2 - \|x_i - a\|^2\right) = \text{sgn}\left(r^2 - D^2\right) \quad (22)$$

F. COMPUTATIONAL COMPLEXITY ANALYSIS

The computational complexity of the proposed method was analyzed using the big O notation. The proposed method comprises of three parts, time parameters extraction, SSE calculation, and the hybrid classifier training. The computational complexity of these three parts was analyzed respectively.

The computational complexity of time parameters extraction is equal to $O(fn{\cdot}L)$, where fn is the total number of framed signal, and L is the length of the framed signal.

The computational complexity of SSE calculation is approximate to $O((N-n+1)\cdot n^2+n)$, where N is the length of the segmented signal, and n is the dimension of the phase space.

According to Ref. [40] and Ref. [41], the computational complexity of SVDD and ELM with M training samples are all $O(M^3)$, thus the computational complexity of the hybrid classifier training is $O(2M^3)$.

In summary, the total computational complexity of the proposed method is $O(fn\cdot L + (N-n+1)\cdot n^2 + n + 2M^3)$.

By removing the low-order terms and constant terms, the computational complexity of the proposed method can be approximate to $O((N-n)\cdot n^2 + M^3)$.

III. EXPERIMENTAL APPLICATION

A real high-voltage SF6 circuit breaker was used as the experimental platform. A monoaxial acceleration sensor named as DH131E was used to record vibration signals of the HVCB, whose frequency response was 1-8000Hz and the measure range was 0-500g. Previous research reported that the installation position of the acceleration sensor significantly affects the accuracy of fault diagnosis of HVCBs [42], [43].

Considering the stability and convenience of data acquisition, two principles should be followed for the installation of acceleration sensors: (1) acceleration sensors do not affect operations of HVCBs; (2) the installation positions for acceleration sensors are close to the structures which are mostly concerned. The beam near the operating mechanism is the position for the installation of the acceleration sensor in this study. The experimental platform and the position for the installation of the acceleration sensor are shown in Fig. 7.

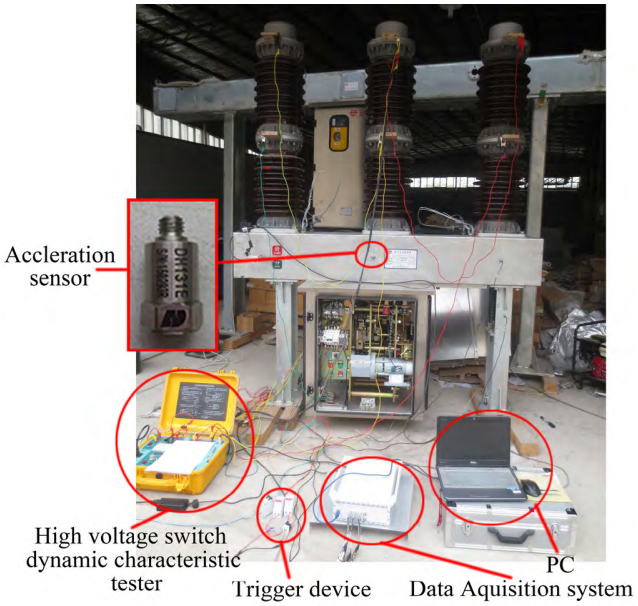

FIGURE 7. Data acquisition system of HVCB.

When receiving the instruction of closing, the data acquisition system starts recording data, with the sampling frequency of 10 kHz and the sampling time period of 300ms. Three types of mechanical faults: invalidation of the buffer spring (Fault I), looseness of the base screw (Fault II), and fault of the actuator (Fault III) were simulated in this study.

These three faults occur frequently in HVCBs and simulated as follows: removal of the buffer spring for the simulation of Fault I, as shown in Fig. 8a; loosening of base screw for the simulation of Fault II, as shown in Fig. 8b; and adjustment of the length of the transmission rod for the simulation of Fault III, as shown in Fig. 8c. In order to prevent damage to the HVCB from excessive operations, 30 samples were collected from each type of faults. Moreover, 30 samples were collected from the Normal State. Furthermore, the contact state and the coil current were recorded using a high

FIGURE 8. Simulation of (a) Fault I. (b) Simulation of Fault II and (c) Fault III.

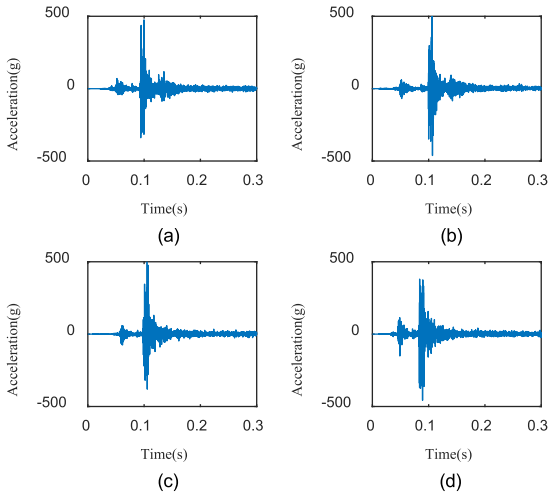

FIGURE 9. Typical waveforms of vibration signals of (a) normal state, (b) Fault I, (c) Fault II, and (d) Fault III.

voltage switch dynamic characteristic tester. Fig. 9 shows typical waveforms of vibration signals of the four different mechanical states.

Analysis of vibration signals of the four different types of states shown in Fig. 9 led to the following conclusions:

The maximum amplitude of Fault I is greater than that of the other types of states, which is due to the fact that the buffer spring does not play a good buffering role.

The starting time of fault III is ahead of the other types of states, which is because of the shortening of the transmission rod. Obviously, these two differences are insufficient to classify faults. More effective features are needed.

IV. RESULTS ANALYSIS

A. EXTRACTION OF MECHANISM ACTION TIME

A vibration signal was first split into 148 frames by Hamming window function with a frame length of 60 points and a frame shift of 20 points. Then STZCR combined with DTM was used to extract mechanism action time of the framed vibration signals. Fig. 10 shows the extraction results, exhibiting that the sub-events are correctly extracted from vibration signals. Time parameters were marked in the form of the vertical lines in Fig. 10. The vertical dotted lines stand for the starting time of a sub-event and the vertical solid lines in Fig. 10 stand for the ending time of a sub-event.

The results were compared with actual time parameters obtained from the contact state and coil current, as shown in Fig. 11. The vertical dotted red lines stand for the actual starting time of sub-events. The black lines stand for time parameters extracted from vibration signals, which have the same meaning as vertical lines in Fig. 10. Moreover, time parameters extracted from vibration signals match up well with actual time parameters.

It appears that the starting time extracted from vibration signals of cam movement is earlier than the actual time while that of the collision of contacts lags behind the actual time. Prior to the action of the cam, the collision caused by the iron core and shackle causes vibration. This affects the extraction results of time parameters of the cam movement. For the collision of contacts, the fact that the acceleration sensor is not located near the vibration source is the reason for the delay time between t3 and t3'.

Comparisons of ending time are limited because of the fact that high voltage switch dynamic characteristic tester cannot get ending time of sub-events.

The maximum error between the extracted time parameters and actual time parameters is listed in Table 1

TABLE 1. The maximum error of time parameters extracted from vibration signals.

States	Error	
	t2	t3
Normal states	4.47%	7.32%
Fault I	6.37%	4.58%
Fault II	4.20%	1.23%
Fault III	1.38%	4.59%

The maximum error of different types of mechanical states is less than 5% in most cases, which illustrates the effectiveness of extraction of time parameters of sub-time from vibration signals.

Using time parameters, a vibration signal can be divided into five segments in the time domain. The first segment and the last segment of the vibration signal are very weak and contain little useful information; therefore, both of them do not participate in the calculation of feature vectors. Fig. 12 shows an example of the segmentation, which is composed of three segments. Every segment can be transformed into a matrix according to (5). Then singular values are obtained by the decomposition of the matrix, which is conducted by SVD. Finally, SSE is calculated according to (7) and (8). The spatial distribution of SSE is shown in Fig. 13.

In previous studies, signals were usually segmented based on equal-time [10] or equal-energy [13] in the process of extracting feature vectors. Following this, SSE was calculated based on equal-time and equal-energy respectively, and the spatial distribution of SSE is shown in Fig. 14.

Obviously, feature vectors shown in Fig. 14(a) and 14(b) are more disordered than those in Fig. 13. Fig. 14 shows obvious aliasing between different states whether for equal-time method or equal-energy method, which indicates that

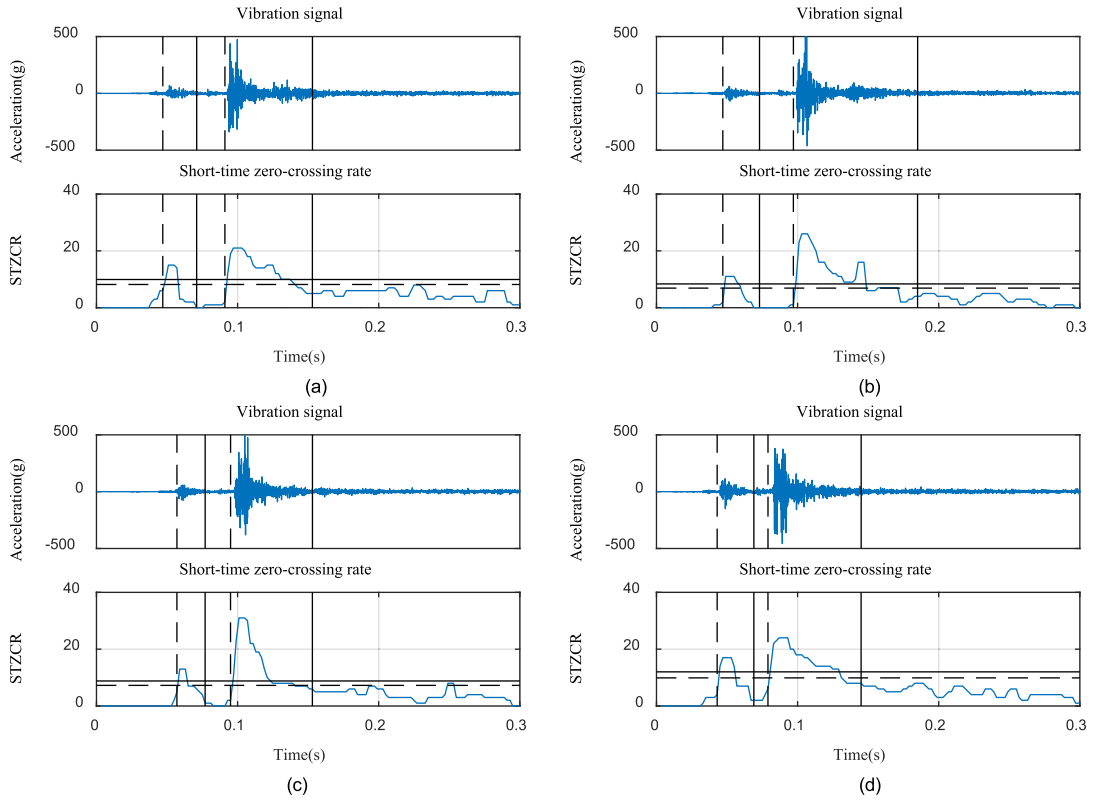

FIGURE 10. Time parameters extracted from vibration signals of (a) normal state, (b) Fault I, (c) Fault II, and (d) Fault III.

TABLE 2. Computational time of different feature extraction methods.

Method	TP-SEE	EMD-EE	VMD-LSVD	EWT-ITFE
Computational time (s)	0.035	0.45	2.74	0.72

segmenting the vibration signal using time parameters is more scientific in the process of calculating SSE.

It is well known that the sooner the fault of HVCBs is detected, the smaller the economic loss. Therefore, it is necessary to monitor the state of HVCBs in real time. In the intelligent diagnosis of HVCBs, feature extraction often consumes a lot of time, especially when signal decomposition is required. Therefore, computational time of three different feature extraction methods used in previous studies was compared in this study. EMD energy entropy (EMD-EE) [16], VMD local singular value decomposition (VMD-LSVD) [15], and EWT improved time-frequency entropy (EWT-ITFE) [13] were calculated to compare computational time. The results are presented in Table 2. TP-SEE in Table 2 was used to refer to the feature extraction method proposed in this study. All experiments were implemented in Matlab 2016b running the computer with a core i7 6700 3.4GHz processor and 4GB RAM. The feature extraction method used in this study takes much less time than the methods reported in literature studies [13], [15], [16], thus it is more in line with the real-time monitoring requirement of the HVCBs.

B. FAULT IDENTIFICATION USING EXTREME LEARNING MACHINE AND SUPPORT VECTOR DATA DESCRIPTION

For comparative analysis, ELM, SVM [14]–[16], BPNN [21], [22], RF [6], [23], FCM [10], and GRNN [13] were all used for the classification of faults of the HVCB, respectively. Moreover, the widely used k-nearest neighbor (KNN) classifier participated in fault diagnosis. These classifiers should be trained first. To compare the performance of these classifiers, 100 trials were conducted to calculate the average diagnosis accuracy. In each test, 24 samples were randomly selected from each state to form the training set and the other 6 samples of each state were grouped into the testing set. The average classification accuracy is listed in Table 3. For better comparison, the results in Table 3 are also illustrated in Fig. 15. Table 3 and Fig. 15 reveal that ELM achieves the highest accuracy of 97.67%, which is significantly higher than that of 91.12%, 75.83%, 89.17%, 92.08%, 87.5%, and 93.33% of SVM, BP, KNN, RF, FCM, and GRNN, respectively. For the identification accuracy of each state, all the classifiers were sensitive to Fault I and Fault III, especially Fault I, which can be completely identified by most classifiers except BP. Noteworthy, FCM can completely identify both Faults I and III, but it has low identification accuracy in Normal state and Fault II. In all classifiers, only ELM maintains high identification accuracy for all states.

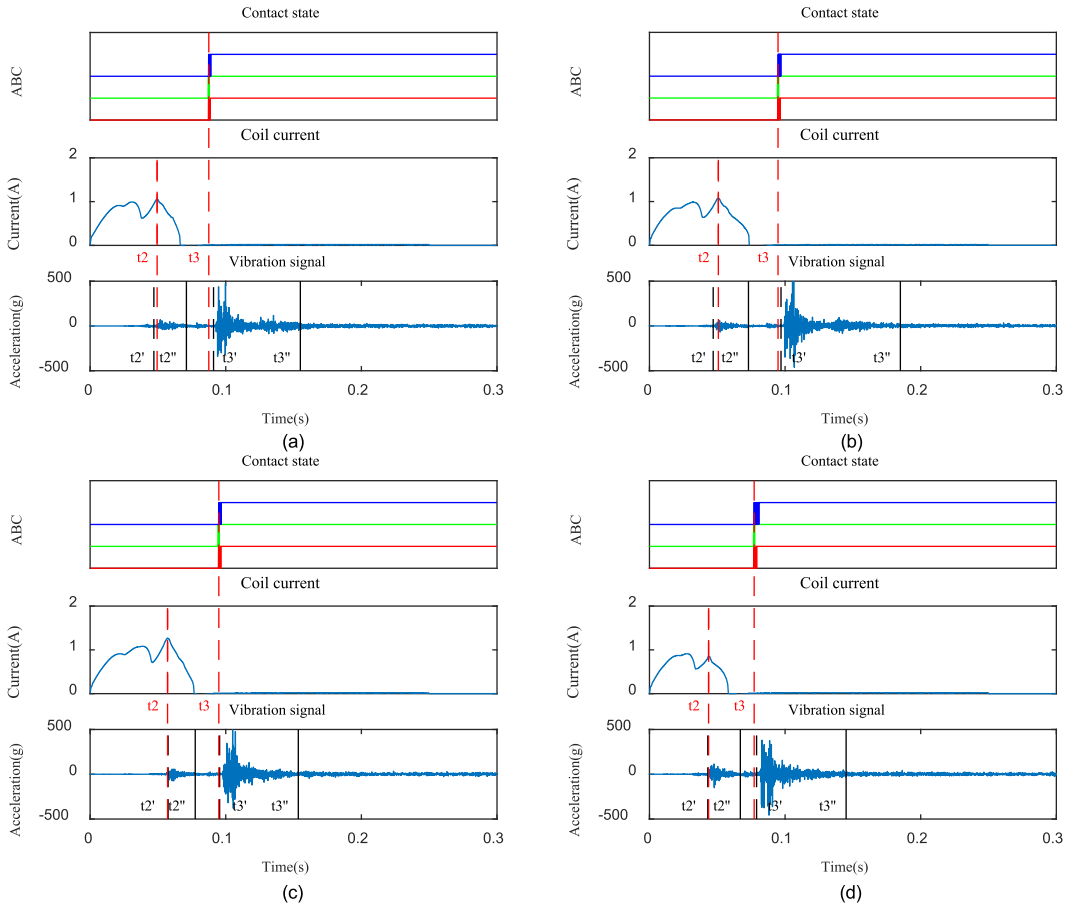

FIGURE 11. Comparison between time parameters extracted from vibration signals and actual time parameters of (a) normal state, (b) Fault I, (c) Fault II, and (d) Fault III.

TABLE 3. Comparative results of seven classifiers.

Classifier	Training time (s)	Testing time (s)	Accuracy (%)				
			Normal state	Fault I	Fault II	Fault III	Overall accuracy
ELM	0.0006	0.0002	95.83	100.00	97.33	97.50	97.67
SVM	0.015	0.013	88.17	100.00	84.33	92.00	91.12
BP	4.26	0.047	60.00	86.67	63.33	93.33	75.83
KNN	0.006.2	0.0014	81.67	100.00	75.00	100.00	89.17
RF	5.86	0.56	85.83	100.00	85.83	96.67	92.08
FCM	0.075	0.0017	73.81	100.00	76.19	100.00	87.50
GRNN	0.028	0.0092	90.83	100.00	88.33	94.17	93.33

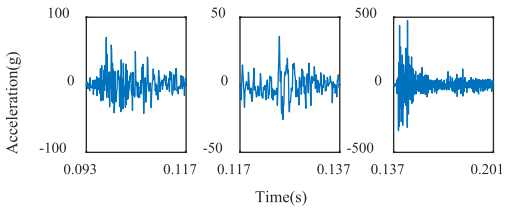

FIGURE 12. Segmental result of a vibration signal of the normal state.

Furthermore, Table 3 summarizes that ELM takes the shortest time for training and testing, which is more useful for real-time diagnosis.

In fact, simulation of all mechanical faults of HVCBs for the training of ELM is unrealistic. Typical multi-class classifiers definitely misclassify unknown faults into known states. It is thus necessary to identify unknown faults before the classification implemented by ELM.

In this study, SVDD was used to detect unknown faults. In order to reflect the performance of SVDD in deferent conditions, Fault I (Case a), Fault II (Case b), and Fault III (Case c) were all assumed to be the unknown fault, respectively. The training set and testing set were constructed in the same way as ELM except that the samples belonging to the unknown faults did not participate in the construction of

TABLE 4. Comparative results of two one-class classifiers of three cases.

classifier	Individual accuracy of Case a (%)			Individual accuracy of Case b (%)			Individual accuracy of Case b (%)		
	Known states	Unknown fault	Overall accuracy	Known states	Unknown fault	Overall accuracy	Known states	Unknown fault	Overall accuracy
SVDD	90.00	100.00	92.50	88.33	100	91.25	88.11	100	91.08
OCSVM	53.33	100.00	65.00	51.67	100	63.75	53.89	100	65.42

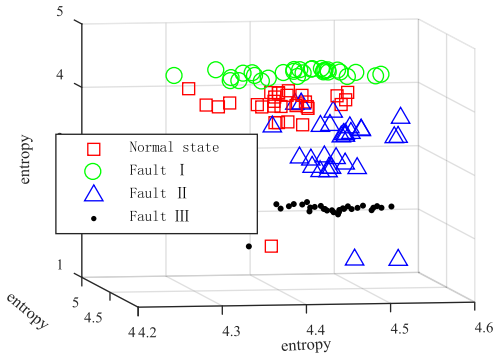

FIGURE 13. Spatial distribution of SSE calculated based on time parameters.

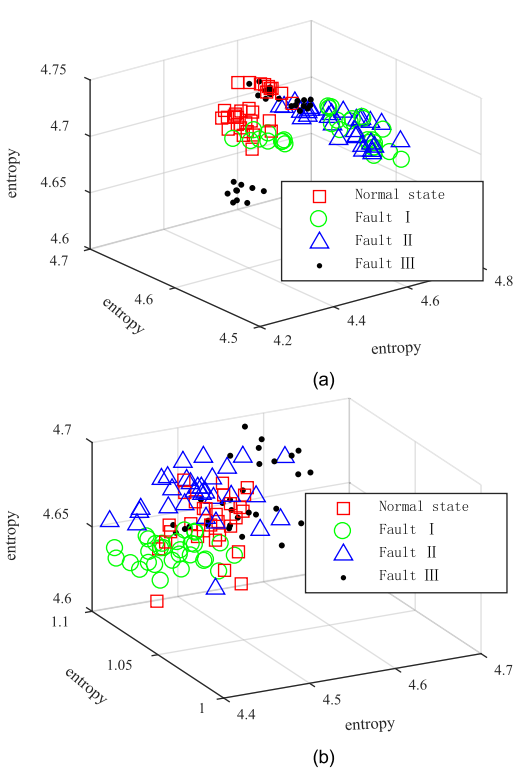

FIGURE 14. Spatial distribution of (a) SSE calculated based on equal-time and (b) SSE calculated based on equal-energy.

the training set. Finally, the testing set was fed into SVDD to test its identification ability for unknown faults. Specifically, the training set has 72 samples belonging to three mechanical states, and the testing set has 24 samples belonging to three mechanical states and the unknown fault. The average identification accuracy was reflected by 100 trials and is presented

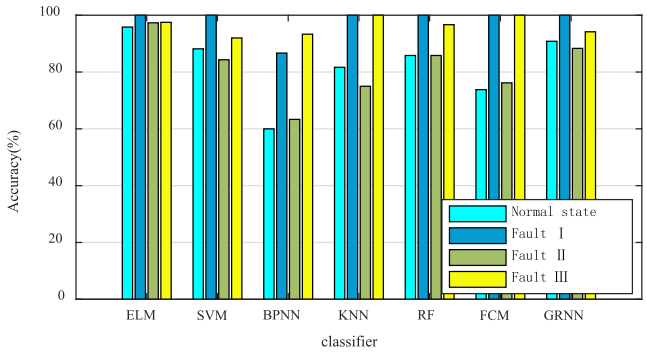

FIGURE 15. Comparative results of seven classifiers.

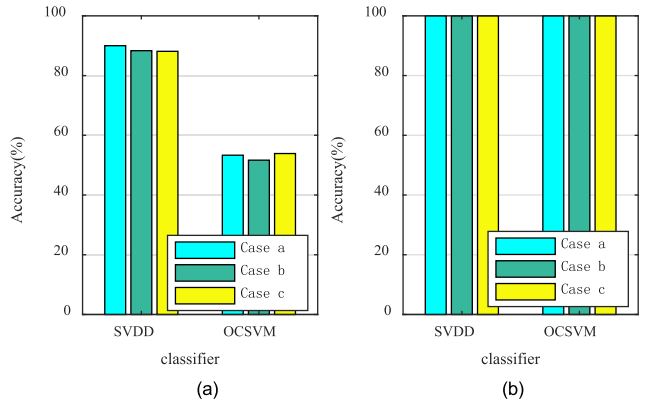

FIGURE 16. Comparison of results between SVDD and OCSVM from perspectives of (a) identification accuracy of known states and (b) identification accuracy of unknown faults.

in Table 4. The identification accuracy of known states and unknown faults was expressed separately. Moreover, the overall accuracy was calculated. For better comparison, results in Table 4 are also illustrated in Fig. 16. Fig. 16(a) illustrates the identification accuracy of known states and Fig. 16(b) illustrates the identification accuracy of the unknown fault.

Table 4 and Fig. 16 indicate that all the samples that belong to the unknown fault of three cases are identified correctly by SVDD. Furthermore, misidentification occurred in known states. If samples belonging to the unknown fault are not successfully detected, they may be classified as the normal state in subsequent state classification, which will be very harmful. It is thus necessary to ensure high identification accuracy of unknown faults in the step of unknown fault detection, even at the expense of the identification accuracy of known states. As a result, the hybrid classifier constructed in this study prioritized the identification of samples belonging

to unknown faults, which is the reason for the high identification accuracy of unknown faults. Furthermore, whether the HVCB was healthy or not was not mistaken, thus the result is acceptable.

Moreover, the superiority of SVDD was verified by the comparison with another one-class classifier, namely, one-class support vector machine (OCSVM). OCSVM can also be used for the identification of unknown faults [14], [44]. Table 4 and Fig. 16 show that all the unknown samples are also identified correctly by OCSVM. However, OCSVM is poor in recognizing known faults, with the accuracy of 53.33%, 51.67%, and 53.89% of three cases, which is much lower than 90.00%, 88.33%, and 91.25% of SVDD, respectively, leading to the overall accuracy of OCSVM far less than that of SVDD. SVDD is thus more suitable for the identification of unknown fault of HVCBs.

V. CONCLUSIONS

This study proposed a novel approach for mechanical faults diagnosis of HVCBs, which can effectively extract precise features from vibration signals and improve the identification accuracy of faults. Mechanism action time was first extracted from vibration signals by STZCR and DTM. Then the raw vibration signals were divided into multiple segments by time parameters. SSE was then calculated as feature vectors from the segmented signals. The hybrid classifier that involved SVDD and ELM was finally employed to identify faults of the HVCB, which could not only classify known states but also identify unknown faults. The main contribution of the method proposed in this study involved the introduction of mechanism action time for feature extraction to improve the diagnosis accuracy and diagnosis speed. The conclusions can be drawn as follows:

(1) Aiming at the difficulty of obtaining the action time of mechanism, a method of extracting the mechanism action time from the vibration signal was proposed in this study. The mechanism action time extracted from vibration signals matched well with the actual mechanism action time.

(2) Compared to equal-time and equal-energy segmentation methods, the segmentation method proposed in this study exhibited superiority in the calculation of feature vectors, resulting in a significant improvement of spatial distribution of feature vectors.

(3) Compared to other classifiers used in previous studies, the hybrid classifier can achieve the highest identification accuracy with the shortest training time. Moreover, the hybrid classifier can precisely detect unknown faults of HVCBs.

Owing to the easiness of the collection of normal samples in the actual operating environment, there is a problem of sample imbalance. Sample imbalance has a high requirement for the classifier and will be studied in future work.

REFERENCES

[1] A. Janssen, D. Makareinis, and C.-E. Sölver, "International surveys on circuit-breaker reliability data for substation and system studies," *IEEE Trans. Power Del.*, vol. 29, no. 2, pp. 808–814, Apr. 2014.

[2] C. R. Heising, A. L. J. Janssen, W. Lanz, E. Colombo, and E. N. Dialynas, "Summary of CIGRE 13.06 working group world wide reliability data and maintenance cost data on high voltage circuit breakers above 63 kV," in *Proc. IEEE Ind. Appl. Soc. Annu. Meeting*, Oct. 1994, pp. 2226–2234.

[3] A. L. Janssen, W. Degen, C. Heising, H. Bruvik, E. Colombo, W. Lanz, P. Fletscher, and G. Sanchis, "Final report of the second international enquiry on high voltage circuit-breaker failures and defects in service," in *Proc. CIGRE Tech. Brochure*, 1994, vol. 83, no. 1, pp. 1–176.

[4] A. A. Polycarpou, A. Soom, V. Swarnakar, R. A. Valtin, R. S. Acharya, V. Demjanenko, M. Soumekh, D. M. Benenson, and J. W. Porter, "Event timing and shape analysis of vibration bursts from power circuit breakers," *IEEE Trans. Power Del.*, vol. 11, no. 2, pp. 848–857, Apr. 1996.

[5] M. Runde, T. Aurud, L. E. Lundgaard, G. E. Ottesen, and K. Faugstad, "Acoustic diagnosis of high voltage circuit-breakers," *IEEE Trans. Power Del.*, vol. 7, no. 3, pp. 1306–1315, Jul. 1992.

[6] S. Ma, M. Chen, J. Wu, Y. Wang, B. Jia, and Y. Jiang, "Intelligent fault diagnosis of HVCB with feature space optimization-based random forest," *Sensors*, vol. 18, no. 4, p. 1221, Apr. 2018.

[7] F. Mei, Y. Pan, K. Zhu, and J. Zheng, "On-line hybrid fault diagnosis method for high voltage circuit breaker," *J. Intell. Fuzzy Syst.*, vol. 33, no. 5, pp. 2763–2774, Oct. 2017.

[8] A. Forootani, A. A. Afzalian, and A. N. Ghohmshe, "Model-based fault analysis of a high-voltage circuit breaker operating mechanism," *Turkish J. Elect. Eng. Comput. Sci.*, vol. 25, no. 3, pp. 2349–2362, May 2016.

[9] Y. Yang, Y. Guan, S. Chen, J. Wang, and K. Zhao, "Mechanical fault diagnosis method of high voltage circuit breaker based on sound signal," *Proc. CSEE*, vol. 38, no. 22, pp. 6730–6737, 2018.

[10] N. Huang, L. Fang, G. Cai, D. Xu, H. Chen, and Y. Nie, "Mechanical fault diagnosis of high voltage circuit breakers with unknown fault type using hybrid classifier based on LMD and time segmentation energy entropy," *Entropy*, vol. 18, no. 9, p. 322, Sep. 2016.

[11] M. Runde, G. E. Ottesen, B. Skyberg, and M. Ohlen, "Vibration analysis for diagnostic testing of circuit-breakers," *IEEE Trans. Power Del.*, vol. 11, no. 4, pp. 1816–1823, Oct. 1996.

[12] M. Liu, K. Q. Wang, L. Sun, and J. Zhen, "Applying empirical mode decomposition (EMD) and entropy to diagnose circuit breaker faults," *Optik*, vol. 126, no. 20, pp. 2338–2342, Oct. 2015.

[13] B. Li, M. Liu, Z. Guo, and Y. Ji, "Mechanical fault diagnosis of high voltage circuit breakers utilizing EWT-improved time frequency entropy and optimal GRNN classifier," *Entropy*, vol. 20, no. 6, p. 448, Jun. 2018.

[14] T. Ji, L. Yi, W. Tang, M. Shi, and Q. H. Wu, "Multi-mapping fault diagnosis of high voltage circuit breaker based on mathematical morphology and wavelet entropy," *CSEE J. Power Energy Syst.*, vol. 5, no. 1, pp. 130–138, Mar. 2019.

[15] N. Huang, H. Chen, G. Cai, L. Fang, and Y. Wang, "Mechanical fault diagnosis of high voltage circuit breakers based on variational mode decomposition and multi-layer classifier," *Sensors*, vol. 16, no. 11, p. 1887, Nov. 2016.

[16] J. Huang, X. Hu, and F. Yang, "Support vector machine with genetic algorithm for machinery fault diagnosis of high voltage circuit breaker," *Measurement*, vol. 44, no. 6, pp. 1018–1027, Jul. 2011.

[17] Q. Zhang, S. Qiao, T. Zhang, and Y. Huang, "Perceptual hashing authentication algorithm for multi-format audio based on energy to zero ratio," *J. Huazhong Univ. Sci. Technol.*, vol. 45, no. 9, pp. 33–38, 2017.

[18] M. Fei, J. Mei, J. Zheng, and Y. Wang, "Development and application of distributed multilayer on-line monitoring system for high voltage vacuum circuit breaker," *J. Elect. Eng. Technol.*, vol. 8, no. 4, pp. 813–823, Jul. 2013.

[19] S. Wan, L. Dou, C. Li, and X. Ma, "Fault diagnosis for high voltage circuit breaker based on timing parameters and FCM," *IEICE Electron. Express*, vol. 15, no. 9, p. 20180227, May 2018.

[20] K. Zhu, F. Mei, and J. Zheng, "Adaptive fault diagnosis of HVCBs based on P-SVDD and P-KFCM," *Neurocomputing*, vol. 240, pp. 127–136, May 2017.

[21] D. S. S. Lee, B. Lithgow, and R. E. Morrison, "New fault diagnosis of circuit breakers," *IEEE Trans. Power Del.*, vol. 18, no. 2, pp. 454–459, Apr. 2003.

[22] M. Liu, B. Li, J. Zhang, and K. Wang, "An application of ensemble empirical mode decomposition and correlation dimension for the HV circuit breaker diagnosis," *Automatika*, vol. 60, no. 1, pp. 105–112, 2019.

[23] S. Ma, M. Chen, J. Wu, Y. Wang, B. Jia, and Y. Jiang, "High-voltage circuit breaker fault diagnosis using a hybrid feature transformation approach based on random forest and stacked auto-encoder," *IEEE Trans. Ind. Electron.*, to be published. doi: 10.1109/TIE.2018.2879308.

[24] A. K. Panda, J. S. Rapur, and R. Tiwari, "Prediction of flow blockages and impending cavitation in centrifugal pumps using support vector machine (SVM) algorithms based on vibration measurements," *Measurement*, vol. 130, pp. 44–56, Dec. 2018.
[25] R. Razavi-Far, S. Chakrabarti, M. Saif, and E. Zio, "An integrated imputation-prediction scheme for prognostics of battery data with missing observations," *Expert Syst. App.*, vol. 115, pp. 709–723, Jan. 2019.
[26] P. Potočnik and E. Govekar, "Semi-supervised vibration-based classification and condition monitoring of compressors," *Mech. Syst. Signal Process.*, vol. 93, pp. 51–65, Sep. 2017.
[27] S. Ding, X. Xu, and R. Nie, "Extreme learning machine and its applications," *Neural Comput. Appl.*, vol. 25, nos. 3–4, pp. 549–556, Sep. 2014.
[28] D. M. J. Tax and R. P. W. Duin, "Support vector data description," *Mach. Learn.*, vol. 54, no. 1, pp. 45–66, Jan. 2004.
[29] F. Meng, S. Wu, F. Zhang, and L. Liang, "Numerical modeling and experimental verification for high-speed and heavy-load planar mechanism with multiple clearances," *Math. Problems Eng.*, vol. 2015, Art. no. 180312, Sep. 2015.
[30] J.-H. Sohn, S.-K. Lee, S.-O. Kim, and W.-S. Yoo, "Comparison of spring models for dynamic analysis of a high voltage circuit breaker with a spring operating mechanism," *Mech. Based Des. Struct. Mach.*, vol. 36, no. 2, pp. 107–128, Apr. 2008.
[31] W.-S. Yoo, S.-O. Kim, and J.-H. Sohn, "Dynamic analysis and design of a high voltage circuit breaker with spring operating mechanism," *J. Mech. Sci. Technol.*, vol. 21, no. 12, pp. 2101–2107, Dec. 2007.
[32] A. A. Razi-Kazemi and M. Abdollah, "Novel high-frequency-based diagnostic approach for main contact assessment of high-voltage circuit breakers," *IET Gener., Transmiss. Distrib.*, vol. 12, no. 5, pp. 1121–1126, Mar. 2017.
[33] Y. Pan, F. Mei, H. Miao, J. Zheng, K. Zhu, and H. Sha, "An approach for HVCB mechanical fault diagnosis based on a deep belief network and a transfer learning strategy," *J. Elect. Eng. Technol.*, vol. 14, no. 1, pp. 407–419, Jan. 2019.
[34] X. Li, S. Wu, X. Li, D. Zhao, and Q. Li, "A study on the dynamic responses and joints clearance optimization of the planar operating mechanism of high-voltage circuit breaker," *Shock Vib.*, vol. 2019, May 2019, Art. no. 9019718.
[35] A. A. R. Kazemi, K. Niayesh, and R. Nilchi, "A probabilistic model-aided failure prediction approach for spring-type operating mechanism of high voltage circuit breakers," *IEEE Trans. Power Del.*, to be published. doi: 10.1109/TPWRD.2018.2881841.
[36] H. Mengyuan, D. Qiaolin, Z. Shutao, and W. Yao, "Research of circuit breaker intelligent fault diagnosis method based on double clustering," *IEICE Electron. Express*, vol. 14, no. 17, Aug. 2017, Art. no. 20170463.
[37] X. Kong, X. Xu, Z. Yan, S. Chen, H. Yang, and D. Han, "Deep learning hybrid method for islanding detection in distributed generation," *Appl. Energy*, vol. 210, pp. 776–785, Jan. 2018.
[38] G.-B. Huang, Q.-Y. Zhu, and C.-K. Siew, "Extreme learning machine: Theory and applications," *Neurocomputing*, vol. 70, nos. 1–3, pp. 489–501, Dec. 2006.
[39] J. Zhou, W. Fu, Y. Zhang, H. Xiao, J. Xiao, and C. Zhang, "Fault diagnosis based on a novel weighted support vector data description with fuzzy adaptive threshold decision," *Trans. Inst. Meas. Control*, vol. 40, no. 1, pp. 71–79, Jun. 2016.
[40] C. S. Chu, I. W. Tsang, and J. T. Kwok, "Scaling up support vector data description by using core-sets," in *Proc. IEEE IJCNN*, Jul. 2004, pp. 425–430.
[41] A. Iosifidis, A. Tefas, and I. Pitas, "Approximate kernel extreme learning machine for large scale data classification," *Neurocomputing*, vol. 219, pp. 210–220, Jan. 2017.
[42] S. Wan, L. Chen, L. Dou, and J. Zhou, "Mechanical fault diagnosis of HVCBs based on multi-feature entropy fusion and hybrid classifier," *Entropy*, vol. 20, no. 11, p. 847, Nov. 2018.
[43] Q. Yang, J. Ruan, Z. Zhuang, D. Huang, and Z. Qiu, "A new vibration analysis approach for detecting mechanical anomalies on power circuit breakers," *IEEE Access*, vol. 7, pp. 14070–14080, 2019.
[44] L. Lin, B. Wang, J. Qi, L. Chen, and N. Huang, "A novel mechanical fault feature selection and diagnosis approach for high-voltage circuit breakers using features extracted without signal processing," *Sensors*, vol. 19, no. 2, p. 288, Jan. 2019.

SHUTING WAN was born in Shanxi, China, in 1971. He received the Ph.D. degree in electrical engineering from North China Electric Power University, Baoding, China, in 2006, where he is currently a Professor with the Department of Energy, Power, and Mechanical Engineering. His research interests include condition monitoring and fault diagnosis of power equipment.

LEI CHEN was born in Linyi, China, in 1993. He received the B.S. degree in mechanical engineering from North China Electric Power University, Baoding, China, in 2016, where he is currently pursuing the Ph.D. degree with the Department of Energy, Power, and Mechanical Engineering. His research interest includes fault diagnosis of power equipment.